Geometric control of human stem cell morphology and differentiation†

Leo Q. Wan,[a] Sylvia M. Kang,[a] George Eng,[a] Warren L. Grayson,[a] Xin L. Lu,[a] Bo Huo,[a] Jeffrey Gimble,[b] X. Edward Guo,[a] Van C. Mow[a] and Gordana Vunjak-Novakovic*[a]

Received 17th March 2010, Accepted 30th June 2010
DOI: 10.1039/c0ib00016g

During tissue morphogenesis, stem cells and progenitor cells migrate, proliferate, and differentiate, with striking changes in cell shape, size, and acting mechanical stresses. The local cellular function depends on the spatial distribution of cytokines as well as local mechanical microenvironments in which the cells reside. In this study, we controlled the organization of human adipose derived stem cells using micro-patterning technologies, to investigate the influence of multi-cellular form on spatial distribution of cellular function at an early stage of cell differentiation. The underlying role of cytoskeletal tension was probed through drug treatment. Our results show that the cultivation of stem cells on geometric patterns resulted in pattern- and position-specific cell morphology, proliferation and differentiation. The highest cell proliferation occurred in the regions with large, spreading cells (such as the outer edge of a ring and the short edges of rectangles). In contrast, stem cell differentiation co-localized with the regions containing small, elongated cells (such as the inner edge of a ring and the regions next to the short edges of rectangles). The application of drugs that inhibit the formation of actomyosin resulted in the lack of geometrically specific differentiation patterns. This study confirms the role of substrate geometry on stem cell differentiation, through associated physical forces, and provides a simple and controllable system for studying biophysical regulation of cell function.

Introduction

Morphogenesis, a biological process of forming a tissue or a whole organism, takes place throughout normal development and adult life, *in vitro* cell culture, and *in vivo* tumor formation. During tissue morphogenesis, cells exhibit collective behaviors such as convergence, extension, invagination and cleft formation. The morphogenetic responses, which involve spatiotemporal changes in cell shape, proliferation, and differentiation, are thought to be controlled by growth factors ('morphogens') which are in turn regulated by gene expression.[1–4] Physical forces play an equally important role in morphogenesis, as demonstrated by abnormal axis formation resulting from mechanical manipulation of embryos[1] and impaired heart chamber and valve formation due to occluded blood flow,[2] to mention just a few examples. The geometry of newly forming tissues and organs and the associated mechanical stresses that are being generated regulate cellular morphology, proliferation and differentiation *via* acting cytoskeletal forces.[3–5]

With recent progress in micro- and nano-technology, geometric regulation of cellular function has been studied at various levels of scale (molecular, cellular, tissue, organ) and in various contexts (development, regeneration, disease).

At a single cell level, cell apoptosis, proliferation and differentiation could be controlled by the cell size and shape,

[a] *Department of Biomedical Engineering, Columbia University, 351 Engineering Terrace, 1210 Amsterdam Avenue, Mail Code: 8904 New York, NY 10027, USA. E-mail: gv2131@columbia.edu; Fax: 212-305-4692; Tel: 212-305-2304*
[b] *Pennington Biomedical Research Center, Louisiana State University, Baton Rouge, LA, 70808, USA*

† Electronic supplementary information (ESI) available: Fig. S1: Frequency maps of osteogenic differentiation (A) and adipogenic differentiation (B) of human adipose-derived stem cells (hASCs) in 1 : 1 mixture of osteogenic and adipogenic media for 4 days; Fig. S2: Alkaline phosphatase activity (ALP) of human adipose-derived stem cells (hASCs) on rectangles (2,000 × 100 μm) in osteogenic differentiation medium for 3 days. See DOI: 10.1039/c0ib00016g

Insight, innovation, integration

We investigated geometric factors associated with the cultivation of adult human stem cells on well-defined patterns, with respect to cell's decision to undergo self-renewal or differentiation into osteogenic and adipogenic lineages. Cultivation on well defined patterns enabled the variation of cell differentiation state, in a manner dependent on the pattern geometry and spatial position, and in correlation with cell morphology. The underlying role of cytoskeleton was probed by inactivating actomyosin in cultured cells. This simple micro-contact printing technique results in precise cell patterning on an adhesive substrate, and thereby enables study of the effects of positionally dependent biophysical forces on cell function. Such an integration of easy to use technology with cell culture can facilitate study of biophysical regulation of cell differentiation.

and substrate topology.[6–11] At a multi-cellular level, the proliferation pattern of endothelial cells was shown to correlate with the local tensile stress.[12] For human mensenchymal stem cells (hMSC), adipogenic differentiation was shown to be regulated by the shape of underlying substrate, but not by the total area.[13] In a recent study of hMSC differentiation in response to osteogenic and adipogenic cytokines, spatial separation of alkaline phosphatase activity and lipid vacuole formation was observed.[14] The spatial patterns of cellular function were attributed to cytoskeletal tension mediated through the Rho/ROCK (Rho-associated Kinase) signaling pathway.[12,14]

Utilization of specialized and controllable culture environments is critical for better understanding of force-geometry control of cell behavior.[15,16] Cell differentiation at early stages of development is of particular interest, where the influence of cell migration due to changes in cell adhesive properties is less pronounced than at later stages of development. We hypothesized that the geometry of a two-dimensional (2D) cell culture substrate can direct stem cells to proliferate or differentiate into specific lineages, through positionally defined mechanical stress and the resulting morphological changes. To this end, we have studied human adipose-derived mesenchymal stem cells cultured on 2D patterns of different shapes and sizes (rings: 500 or 1000 μm in diameter and 100 or 200 μm wide; rectangles: 500 or 1000 μm long and 100 or 200 μm wide). These geometries were selected because they can provide local conditions representative of the situations during normal development, where cells are subjected to boundaries, to which they respond by proliferation or differentiation in a positionally defined manner. For example, during branching morphogenisis of mouse lung epithelium, the increase of cell proliferation was found at distal sites of newly formed buds, due to the elevated cytoskeletal tension associated with the curvature.[17] We investigated the effects of such patterns on cell decisions, and the role of cytoskeletal tension in cell decisions was further probed using pharmacological treatment, with the goal to elucidate the role of geometry-force related factors on cell differentiation and tissue morphogenesis.

Materials and methods

Microfabrication and microcontact printing

Cells were patterned onto the substrate by micro-contact printing, using self-assembly monolayers (SAMs) and polydimethylsiloxane (PDMS) elastomeric stamp (Fig. 1A).[7,18] First, a mold was fabricated by spin-coating a 100 μm thick film of SU-8 2050 photoresist (MicroChem Corp, Newton, MA) onto silicon wafers, and exposing the photoresist to UV light (Omnicure 1000, EXFO) through a chromium mask with desired geometric features. Rings of various inner diameters (D = 500 or 1000 μm) and widths (W = 100 or 200 μm), and rectangles of different lengths (L = 500 or 1000 μm) and widths (W = 100 or 200 μm) were fabricated. The photoresist was developed in propylene glycol monomethyl ether acetate (Sigma, St. Louis, MO) to remove uncrosslinked polymers. The resulting mold was then immersed into a 10 : 1 mixture of

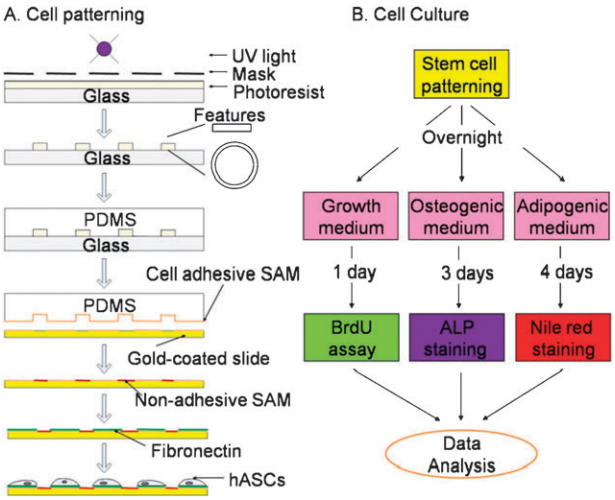

Fig. 1 Experimental design for studying spatial patterns of stem cell function. (A) Micro-fabrication and micro-contact printing for patterning of human adipose-derived stem cells (hASCs). PDMS (polydimethylsiloxane) elastomeric stamps were casted with pre-polymers onto a negative photoresist mold, which was formed with UV (ultraviolet) crosslinking through a mask containing desired small features (rectangles and rings of different sizes). An adhesive self-assembly monolayer (SAM) octadecanethiol was transferred *via* PDMS stamp onto gold-coated glass slides, which were then sequentially subject to a non-adhesive ethylene glycol-terminated SAM HS-$(CH_2)_{11}$-EG_3 and extracellular matrix protein, fibronectin. (B) Cell proliferation, osteogenic and adipogenic differentiation in the corresponding culture medium were examined by BrdU assay, Alkaline phosphatase (ALP) and Nile red staining, respectively.

PDMS pre-polymer and curing agent (Sylgard 184 kit, Dow Corning, Midland, MI) and cured at 70 °C for 4 h before the PDMS was removed from the master.

The PDMS stamp was then used to transfer an adhesive SAM onto gold-coated glass slides through the micro-contact printing technique. The glass slide was sequentially coated with a 15 Å thick titanium adhesion layer and a 150 Å thick gold film using an electron-beam evaporator (Semicore SC200; Livermore, CA). An adhesive SAM octadecanethiol (Sigma) was stamped for 60 s onto the glass surface. The unstamped regions were then subjected to a non-adhesive ethylene glycol-terminated SAM (HS-C_{11}-EG_3, Prochimia, Poland) for 3 h. Finally, patterned surfaces were washed with ethanol and coated with 10 μg/mL fibronectin (Sigma) for 30 min.

Cell culture

Human adipose-derived stem cells (hASCs) were chosen in this study due to their increasing potential for tissue regeneration as an easily accessible cell source.[19] The hASCs were isolated from liposuction aspirates of human subcutaneous adipose tissue.[19] Briefly, liposuction waste tissue was digested using collagenase, and the floating adipocytes were removed from the precipitating stromal fraction by centrifugation. The remaining stromal cells were plated in tissue culture flasks for 4 to 5 days, and the attached cells were harvested and cryopreserved in liquid nitrogen until use. To start an experiment, the cells were thawed, plated in growth medium (high glucose, 10% fetal bovine serum, FBS), grown until confluence, trypsinized, and

seeded onto the patterned fibronectin-coated slides. Patterned cells were cultured in growth medium (with 2% FBS) overnight to form geometrically defined cellular monolayers in which the individual cells could sense positional information.[12] The attached cells were then incubated either in growth medium (2% FBS), or in osteogenic medium (2% FBS, 100 nM dexamethasone, 10 mM β-glycerophosphate, and 0.1 mM acorbic-acid-2-phosphate), or in adipogenic medium (2% FBS, 1 μM dexamethasone, 0.2 mM indomethacin, 0.5 mM methylisobutylxanthine, and 10 μg/mL insulin) (Fig. 1B). In addition, cells were also cultured in 1 : 1 mixed ostogenic and adipogenic media for 4 days before cell staining for each osteogenic and adipogenic differentiation was performed. Cell culture media were changed every other day.

Blocking of Rho/ROCK pathway

To examine the role of cytoskeletal tension and Rho/ROCK signaling pathway in stem cell differentiation, 2 μM Y-27632 (CalBioChem, Darmstadt, Germany), 10 μM ML-7 (CalBioChem), and 5 μM Bebbistatin (Tocris bioscience, Ellisville, MO) were added into the culture medium during cultivation for osteogenic differentiation. Y-27632 is a selective inhibitor of p160-Rho-associated coiled-coil forming protein serine/threonine kinase (ROCK-I).[20] Y-27632 prevents the phosphorylation of myosin regulatory light chain (MRLC). ML-7 is a selective inhibitor of myosin light chain kinase (MLCK).[21] Blebbistatin inhibits nonmuscle myosin II ATPase activity by blocking myosin heads in a complex with low actin affinity.[22]

Assessment of cell proliferation and differentiation

Cell proliferation. Cellular proliferation was accessed by the BrdU assay. Patterned cells were exposed to 10 μM Bromo-deoxyuridine (BrdU) for about 18 h before fixation with 3.7% formalin in PBS for 10 min, and permeated with 2N HCl and 0.5% Triton X-100 in Tris buffered saline (TBS). After incubation with the blocking buffer (2% FBS in TBS) for 2 h, the samples were immersed into the antibody anti-rat BrdU-FITC (Abcam) in blocking buffer for 4 h in a humid chamber at room temperature. The cell nuclei were stained with 200 ng/mL 4′, 6-diamidino-2-phenylindole (DAPI) in PBS for 5 min.

Osteogenic differentiation. To evaluate osteogenic differentiation, the cells were stained for alkaline phosphatase activity after culture following procedure No.85 from Sigma. Cells were fixed with 60% citrate buffered acetone for 45 s, rinsed with water for 30 s, and immediately incubated in Fast Blue RR/Naphthol solution at room temperature. After 30 min, glass slides were rinsed with water, and bright-field images of cells were then photographed under microscope.

Adipogenic differentiation. To evaluate adipogenic differentiation, cultured cells were fixed with 3.7% formalin for 10 min, rinsed with PBS, and stained with 1μg/mL Nile red (dissolved in acetone) in PBS. Fluorescence images (Texas red) were taken for oil droplets inside differentiated cells with an inverted fluorescence microscope (Olympus) with a Hamamatsu CCD camera.

Quantitative analysis of cell differentiation patterns

Immunostained images of osteogenic cells (expressing alkaline phosphatase, ALP) and adipogenic cells (forming oil droplets) were segmented by thresholding of color intensity in patterned cells. At each pixel, the probability of cell differentiation was calculated in ≥ 40 individual images, and color-coded using the "jet" colormap in MatLab (MathWorks, Natick, MA). For cells on ring patterns, the probability was averaged along the circumferential direction, and the radial differentiation profile was then obtained between the inner and outer rings. For cells on rectangles, linear differentiation profiles were obtained along both length axes.

Analysis of cell and nucleus morphology

The phase contrast images of the patterned cells were taken right after overnight culture in growth medium. This time point was chosen because the overnight culture provided sufficient time for cell spreading, contacting with neighboring cells, and sensing of the geometry of substrate, without the use of cytokines that would affect cell morphology. Due to the symmetry of the ring patterns, cell morphology on the rings with an inner diameter of $D = 1000$ μm and a width of $W = 200$ μm were quantified using ImageJ (NIH, Bethesda, MD). The boundary of each cell was outlined manually, and the projected area of the cell was calculated as the total area enclosed by the cell boundary. The cell aspect ratio was determined using the "Fit ellipse" tool and calculated as the ratio of the primary (major) and secondary (minor) axes of the ellipse that provided the best fit for the selected cells. A perfectly circular cell would have an aspect ratio of 1, while elongated cells would have aspect ratios of >1. Cell nuclei were analyzed in a similar way, for DAPI stained cells on ring patterns.

Statistics

The stem cell ALP activity was first averaged along the two axes for rectangles and in the radial direction for rings. A Student t-test was performed at a level of significance $\alpha = 0.05$ to detect spatial variations in ALP expression for the two geometries of various sizes.

For cell morphological analysis, the ring patterns were further divided into five sub-rings of equal width (40 μm), and each cell was classified into one of the five sub-regions based on the radial location of its centroid. The cell area and aspect ratio were calculated as an average ± standard error. One-way ANOVA tests were performed to evaluate the dependence of geometric parameters on radial position, with a Tukey-Kramer post hoc test at $\alpha = 0.05$.

Results

Human adipose-derived stem cells (hASCs) readily attached to fibronectin-coated areas on glass slides within 1–2 h after seeding, migrated and formed continuous monolayers over the entire micro-patterned surface after overnight cultivation. The highest rate of cell proliferation was observed at the outer edge of the ring patterns, and along the short axes of the rectangle patterns, as indicated by BrdU incorporation and

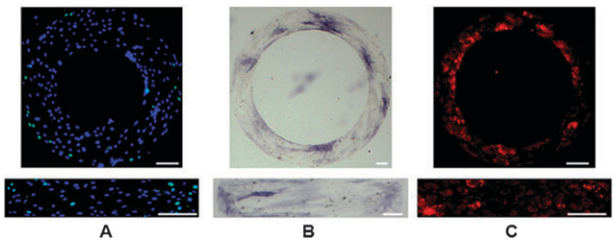

Fig. 2 Localization of stem cell proliferation and differentiation. (A) Combined fluorescence images of stem cell proliferation on ring and rectangular patterns in growth medium for 1 day (Green: Bromodeoxyuridine (BrdU); Blue: nuclei); (B) Bright field images of Alkaline phosphatase staining (with Fast Blue dye) of human adipose derived stem cells (hASCs) after 3 days incubation in osteogenic medium; (C) fluorescence images of Nile red staining of lipid droplets inside hASCs after cultured in adipogenic medium for 4 days. Scale bars: 100 μm.

subsequent fluorescence labeling (Fig. 2A). Osteogenic differentiation (by Fast Blue RR/Naphthol staining of ALP) and adipogenic differentiation (by Nile Red staining of lipid droplets) confirmed the multi-potency of each batch of cells used in the experiments. Notably, the regions expressing elevated ALP activity in osteogenic medium, as indicated by strong expression of ALP at the inner edge of the rings and adjacent to the short axis edges of rectangles, were complementary to the regions of cell proliferation (Fig. 2B). Lipid droplets inside cells under adipogenic differentiation conditions were found in these same regions (Fig. 2C).

To quantify the spatial distribution of cell differentiation, the immunostains were evaluated based on color intensity. An example of such analysis is shown for ALP staining of stem cells cultured for 3 days in osteogenic medium on a ring pattern (D = 500 μm, W = 200 μm, Fig. 3A-1). The image was segmented based on color, by selecting the pixels denoting ALP activity sites, which are shown by dark regions (Fig. 3A-2). The accuracy of this procedure was confirmed in the overlaid images (Fig. 3A-3), formed by co-localization of the ALP stain (Fig. 3A-1) and dark color (Fig. 3A-2). The frequency maps were generated using ≥ 40 segmented binary images for each experimental group and time point, to determine the probability of stem cell differentiation at each pixel within the pattern, for each shape, size, and time point.

For ring patterns, the ALP activity of stem cells during osteogenic differentiation decreased with radius from the inner to the outer ring (Fig. 3B-1). For rectangular patterns, the strongest ALP staining appeared in the regions close to the short axis edges, as compared to the center of rectangle and the very edges (Fig. 3B-2). Similar but less distinctive patterns of oil droplets were found for small size patterns expressing adipogenic differentiation (Fig. 3B-3 and 4). The difference between inner ring and outer ring, however, was still statistically significant ($p < 0.05$). In addition, ALP and Nile Red stainings of cells in osteogenic and adipogenic mixed media revealed similar differentation patterns (Fig. S1, ESI†). All differentiation patterns were able to maintain for a prolonged time culture (up to 6–7 days when these highly metabolically active cells started to migrate out of patterned geometries) with an evaluted overall level of differentiation.

Phase contrast images showed that the cells cultured on ring patterns aligned predominantly in the circumferential direction and had large projected areas at the outer region, as compared to the elongated cells with small projected areas at the inner ring (Fig. 3C-1). On rectangular patterns, cells with large projected areas were observed mostly at the corners and at the short edges of rectangles, while the elongated cells with small projected areas were observed at the regions close to short edges (Fig. 3C-2).

Morphological parameters of the cells cultured on rings were analyzed as a function of the radial position (Fig. 3D). For a ring with an inner diameter of D = 1000 μm and a width of W = 200 μm, there were approximately 400 cells on each pattern. The average size of the cells increased from $\sim 1460 \pm 90$ μm^2 (mean ± standard error) at the inner ring to $\sim 1970 \pm 140$ μm^2 at the outer ring ($p < 0.05$). Cell nuclei at the edges tended to be smaller than in the interior regions (208 ± 6 μm^2 *vs.* 230 ± 8 μm^2), but the differences were not significant. ($p > 0.05$). Cells with larger aspect ratios (AR = 7.4 ± 0.3) were found near the inner and outer regions of rings, as compared to the center region (AR = 5.2 ± 0.2) ($p < 0.05$). A similar trend was found for the aspect ratio of the cell nucleus with AR = 1.84 ± 0.03 at the edges and AR = 1.64 ± 0.03 at the center ($p < 0.05$).

At small rectangular patterns (length of ≤ 500 μm, width of 100 μm), cell differentiation occurred mostly at the middle of the rectangles, whereas at the larger patterns (length of 500–1000 μm, with of 100–200 μm), differentiated cells were concentrated in regions close to the two short edges of the rectangles (Fig. 4A). The rectangle with a large aspect ratio (2000 μm in length and 100 μm in width) was also tested and the cells exhibited a similar differentiation pattern (Fig. S2, ESI†). When the width of the rectangle increased from 100 μm to 200 μm, the polarization of stem cell differentiation became more evident. For rings (Fig. 4B), the increase in the inner ring diameter from 500 μm to 1000 μm elevated ALP activity at the inner ring region, whereas the increase of the ring width from 100 to 200 μm decreased the level of ALP activity.

To directly test the possible role of cytoskeletal tension in the observed patterns of stem cell differentiation, three different inhibitors of the Rho/ROCK pathway were employed. When cells were exposed to Blebbistatin (myosin II ATPase inhibitor), ML-7 (MLCK inhibitor) or Y-27632 (ROCK inhibitor), the level of osteogenic differentiation decreased, and more importantly, the pattern of stem cell differentiation (gradient along the radial direction) on rings became less distinctive (Fig. 5). These effects of the three drugs known to inhibit actomyosin formation suggest that the observed cell differentiation patterns can be attributed, at least in part, to cytoskeletal tension associated with cell shape.

Discussion

Our objective was to investigate how the geometry of cell monolayers regulates local cellular function. Using micropatterning techniques, we show that the proliferation and differentiation of human adult stem cells (hASCs, isolated from adipose tissue aspirates) can be modulated by substrate

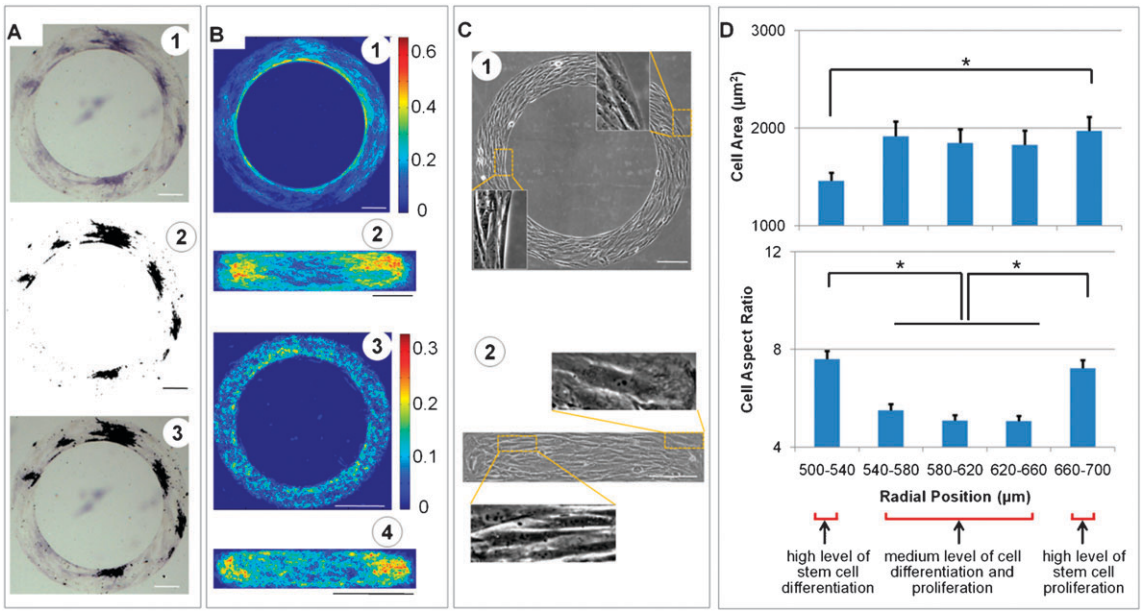

Fig. 3 Cell differentiation maps and cell morphology. (A) Image processing for the distribution of alkaline phosphatase (ALP) activity of stem cells cultured for 3 days on a ring pattern in osteogenic medium. High AKP activity is shown by purple in bright field images (A1), black in thresholded images (A2), and the dark regions in overlaid images (A3). The probability of cell differentiation was calculated at each pixel by averaging multiple binary images (A2) (n = 40–80) and the frequency maps were then generated as shown for ALP expression (B 1-2) in stem cells in osteogenic medium, and for lipid droplets in adipogenic medium (B3-4). (C) Phase contrast images of cells on micropatterns. Cells at the outer regions of rings and the corners of rectangles are shown with a larger projection area, while cells at inner rings and regions close to short edges of rectangles are smaller and narrower. (D) Morphological analysis of cells on rings (inner diameter: 500 μm; width: 200 μm) as a function of the radial position. Cell differentiation colocalized with the small size and large aspect ratio of the cultured cells (*$p < 0.05$). Scale bars: 200 μm.

geometry. Cell proliferation was enhanced in specific areas occupied by large, spreading cells (*e.g.*, outer ring and corners of rectangles), while cell differentiation was observed at different regions with elongated cells having a relatively small projected area (*e.g.*, inner ring and regions close to short edges of rectangles). The use of pharmacological agents blocking the actomyosin confirmed that cytoskeletal tension played a role in the observed geometric regulation of stem cell shape and differentiation. Taken together, these data suggest that stem cell function can be regulated by the geometry of multi-cellular patterning, through geometry-derived forces affecting cell morphology and cytoskeletal organization.

High cell proliferation rates at the corners and short edges of rectangles and the outer edges of the rings (Fig. 2A) were consistent with previous findings for highly adhesive endothelial cells[12] and less adhesive NIH 3T3 fibroblasts.[23] Morphological analysis showed that proliferating cells had large projected areas (Fig. 3C). Large cytoskeletal tension or traction forces[12,14,23] may account for the large cell size and high proliferation rate, while low levels of cytoskeletal tension resulting from increased cell–cell contacts[24,25] may account for the inhibition of cell proliferation. Consistently, the regions with large spreading cells had the lowest levels of osteogenic and adipogenic differentiation (Fig. 3–4). Instead, cell proliferation was inhibited and differentiation was enhanced in regions with small, elongated cells (the inner edge of rings, regions close to short edges of rectangles, and the interior regions of the small rectangles in which the cells were subjected to relatively high stresses). Consequently, cell proliferation and cell differentiation were essentially separated on all of our geometries.

We have observed similar cell differentiation patterns for early differentiation (3–4 days) of hASCs in either osteogenic medium, adipogenic medium, or 1 : 1 osteogenic/adipogenic medium. Our finding that adipogenic differentiation located at the inner ring region is consistent with that found in a previous long-term (2 week) study of cells cultured in cocktail medium with cytokines for osteogenic and adipogenic differentiation.[14] However, in contrast to this previous study, we found that the regions with adipogenic differentiation on rectangular patterns were located close to short edges (instead at the center as in the previous study[24]). Our result appears consistent with another recent study which focused on the overall level of early adipogenic differentiation of hMSCs on 2D geometries,[13] which is also comparable to ours with the number of lipid droplets inside cells. In addition, high osteogenic differentiation was not observed in the outer ring as found by Ruiz and Chen,[14] but instead in the inner ring.

These apparently inconsistent cellular responses may be indicative of different effects of geometry-induced mechanical forces on cultured cells at different times of culture. We thus propose that the geometry of cellular patterns may induce cell sensitivity to soluble cues early in differentiation, rather than driving differentiation towards a specific lineage.

The observed patterns of cell morphology and differentiation are likely related to the cytoskeletal tension rearrangements

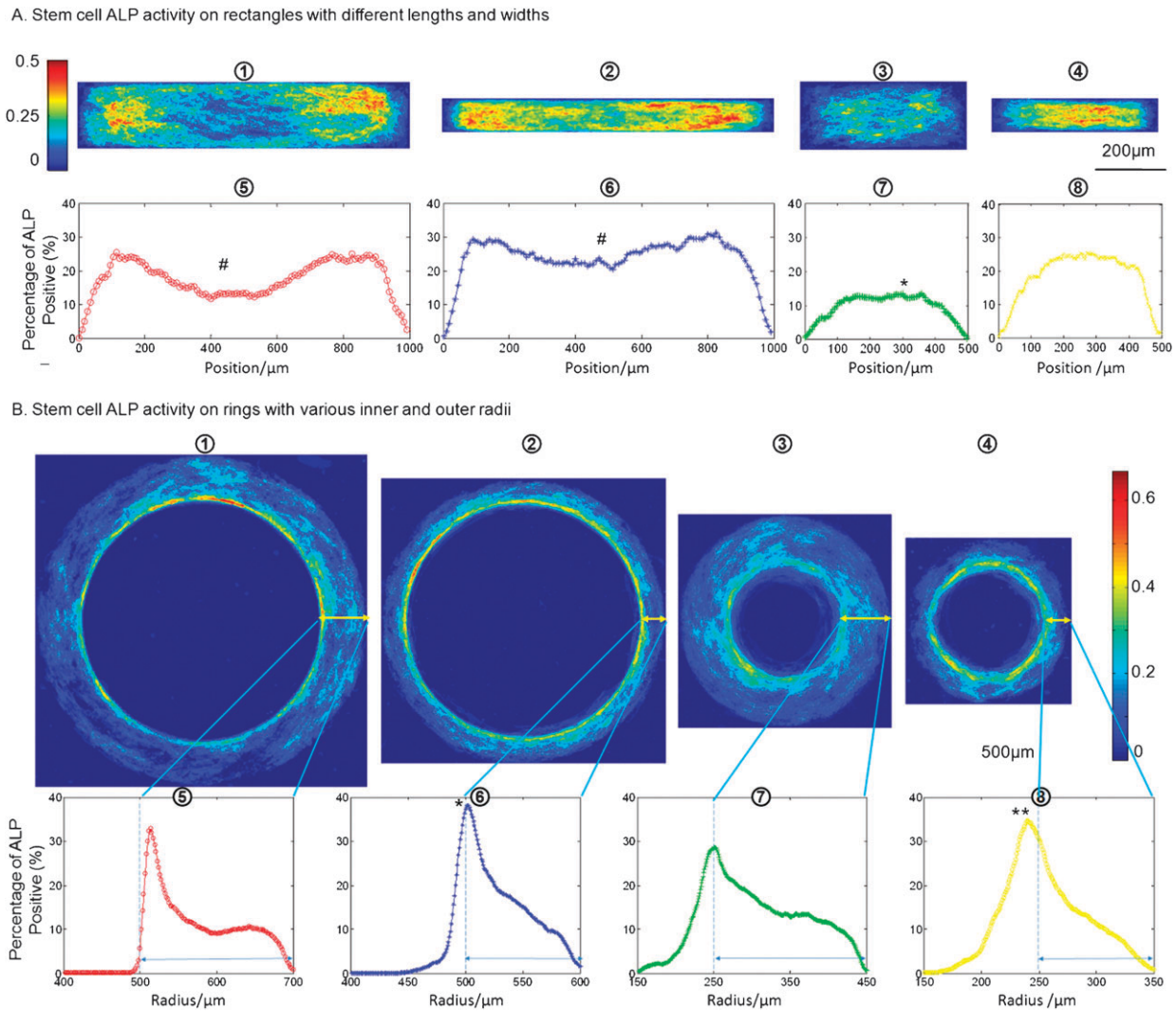

Fig. 4 Dependence of stem cell differentiation frequency maps on pattern geometry. (A) ALP activity of human adipose-derived stem cells (hASCs) in osteogenic differentiation medium for 3 days. Frequency maps (1–4) of ALP activity are shown for stem cells on rectangles measuring 1000 × 200 μm, 1000 × 100 μm, 500 × 200 μm, and 500 × 100 μm; the corresponding average ALP activity along the length of each pattern is shown in 5–8. (B) ALP activity of hASCs on rings. Stem cell ALP activities on ring patterns with different sizes are shown in the frequency maps (from left to right 1–4: inner diameter D = 1000 μm, width W = 200 μm; D = 1000 μm, W = 100 μm; D = 500 μm, W = 200 μm; and D = 500 μm, W = 100 μm), and the corresponding ALP activity profile across the radius is shown in 5–8. Double-ended arrows indicate the patterned cell-adhesive regions. (# significantly different from the peak ALP activity near two ends in the same rectangle, * significantly from other groups, and ** significantly different from the ring with an inner diameter of 500 μm and width of 200 μm; $p < 0.05$).

resulting from cell–cell and cell-substrate interactions. It is established that the adhesive bonds between cells (*e.g.*, *via* adherent junctions) and the aggregate surface tension (*e.g.*, *via* tensile stresses in cell membrane and microfilament bundles along cell boundary) can act as an internal attractive force and bring cells closer to each other.[26–29] The mechanical tension generated at cell–cell contacts can be further transmitted through the cytoskeletal network and balanced internally by the newly formed actin-myosin motors. The pharmacological treatment with Y-27632, ML-7, and Blebbistatin (Fig. 5) can not only decrease cytoskeletal tension but also disrupt force transmission between cells by reducing cellular stress fiber formation and cell contractility. The diminishing patterns (*i.e.*, gradient across the radius of rings) of stem cell differentiation further support the role of cytoskeletal tension and cell–cell interaction in stem cell differentiation. Similarly, the less distinct adipogenesis patterns, compared to the osteogenesis ones, could also be related to the disruption of force transmission due to the decrease in cell size and loss of cell–cell contact under adipogenic induction. As a result, the cells could not sense their positional information and behaved more like single cells.

Similar patterns observed for osteogenic and adipogenic differentiation (Fig. 3B) despite of the difference in their epigenetic regulation (*e.g.*, substrate stiffness and cell morphology[10,30]) indicate that at early stages of stem cell differentiation, cellular morphological changes due to geometric control may cause the activation of stem cell sensitivity to regulatory cues such as soluble growth factors in culture media rather than promote specific stem cell differentiation paths. In an attractor

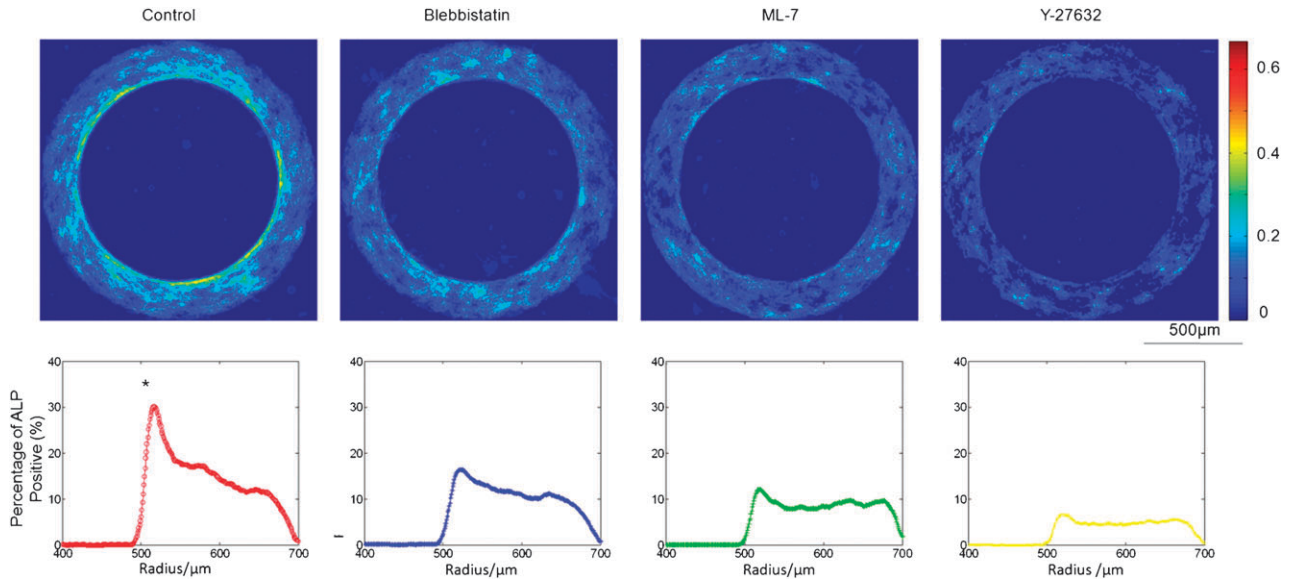

Fig. 5 The role of cytoskeleton. Disruption of cytoskeletal tension diminished the patterns of geometrically controlled osteogenic differentiation of hASCs. The frequency maps (top) of ALP activities are shown for stem cells on ring patterns (inner radius: 500 μm and width: 200 μm) after 3 days incubation (from left to right) in osteogenic medium (control) and in osteogenic medium with addition of 10 μM Blebbistatin, 10 μM ML-7, or 2 μM Y-27632. The corresponding cell ALP activities across the radius are shown below the frequency maps. (* significantly different from other groups in the peak ALP activity; $p < 0.05$).

landscape presentation of cell fate,[31] the activated cytoskeleton may thus act as a stimulus for cells to leave a quiescent state before falling into other basins of attraction such as differentiation and proliferation.

The cultivation of stem cells on geometric patterns had markedly different effects on cell differentiation and proliferation, and is consistent with differential regulation of these two functions by physical signals in cellular micro-environment. At a multi-cellular level, a finding similar to ours has been reported for endothelial cells on intermediate size patterns, that were shown to switch into the differentiation mode and form capillary tubes,[32] as compared to apoptosis on small patterns, and high proliferation on large patterns.

Although the exact underlying mechanism is not known, cell–cell interaction seems necessary for geometric regulation of stem cell differentiation. Without cell–cell interaction, the cell size effect on the rate of keratinocyte differentiation was negligible.[33] In contrast, cell–cell contacts promoted the keratinocyte differentiation as indicated with enhanced involucrin and keratin 10 expression.[33] Likewise, a proper initial cell seeding density was also crucial for establishing distinct differentiation patterns in our study. A well designed experiment to independently control cell morphology and cell–cell contact may give more insights in how stem cell differentiation can be regulated at different locations within the geometries. In addition, further studies are necessary for determining the signaling pathway of mechanotransduction and detailed stress analysis on cell–cell and cell-substrate interaction in such a multi-cellular system.

In summary, cell function can be regulated by substrate patterning. Human adipose-derived stem cells differentiated and proliferated in different regions of cell culture patterns in a manner dependent on pattern geometry, local position and the acting biophysical forces.

Acknowledgements

We gratefully acknowledge NIH funding of this work (grant EB002520).

Notes and references

1 L. V. Belousov and A. S. Ermakov, *Ontogenez*, 2001, **32**, 288–294.
2 J. R. Hove, R. W. Koster, A. S. Forouhar, G. Acevedo-Bolton, S. E. Fraser and M. Gharib, *Nature*, 2003, **421**, 172–177.
3 L. Hufnagel, A. A. Teleman, H. Rouault, S. M. Cohen and B. I. Shraiman, *Proc. Natl. Acad. Sci. U. S. A.*, 2007, **104**, 3835–3840.
4 B. I. Shraiman, *Proc. Natl. Acad. Sci. U. S. A.*, 2005, **102**, 3318–3323.
5 R. Gordon, *Int. J. Dev. Biol.*, 2006, **50**, 245–253.
6 G. H. Altman, R. L. Horan, I. Martin, J. Farhadi, P. R. Stark, V. Volloch, J. C. Richmond, G. Vunjak-Novakovic and D. L. Kaplan, *Faseb J*, 2002, **16**, 270–272.
7 C. S. Chen, M. Mrksich, S. Huang, G. M. Whitesides and D. E. Ingber, *Science*, 1997, **276**, 1425–1428.
8 M. J. Dalby, N. Gadegaard, R. Tare, A. Andar, M. O. Riehle, P. Herzyk, C. D. Wilkinson and R. O. Oreffo, *Nat. Mater.*, 2007, **6**, 997–1003.
9 D. E. Ingber, *Proc. Natl. Acad. Sci. U. S. A.*, 1990, **87**, 3579–3583.
10 R. McBeath, D. M. Pirone, C. M. Nelson, K. Bhadriraju and C. S. Chen, *Dev. Cell*, 2004, **6**, 483–495.
11 S. Oh, K. S. Brammer, Y. S. Li, D. Teng, A. J. Engler, S. Chien and S. Jin, *Proc. Natl. Acad. Sci. U. S. A.*, 2009, **106**, 2130–2135.
12 C. M. Nelson, R. P. Jean, J. L. Tan, W. F. Liu, N. J. Sniadecki, A. A. Spector and C. S. Chen, *Proc. Natl. Acad. Sci. U. S. A.*, 2005, **102**, 11594–11599.
13 W. Luo, S. R. Jones and M. N. Yousaf, *Langmuir*, 2008, **24**, 12129–12133.
14 S. A. Ruiz and C. S. Chen, *Stem Cells*, 2008, **26**, 2921–2927.
15 D. O. Freytes, L. Q. Wan and G. Vunjak-Novakovic, *J. Cell. Biochem.*, 2009, **108**, 1047–1058.
16 G. Vunjak-Novakovic, *Cell Stem Cell*, 2008, **3**, 362–363.
17 H. Nogawa, K. Morita and W. V. Cardoso, *Dev. Dyn.*, 1998, **213**, 228–235.

18 X. E. Guo, E. Takai, X. Jiang, Q. Xu, G. M. Whitesides, J. T. Yardley, C. T. Hung, E. M. Chow, T. Hantschel and K. D. Costa, *Mol. Cell Biomech*, 2006, **3**, 95–107.
19 Y. D. Halvorsen, D. Franklin, A. L. Bond, D. C. Hitt, C. Auchter, A. L. Boskey, E. P. Paschalis, W. O. Wilkison and J. M. Gimble, *Tissue Eng.*, 2001, **7**, 729–741.
20 T. Ishizaki, M. Uehata, I. Tamechika, J. Keel, K. Nonomura, M. Maekawa and S. Narumiya, *Mol. Pharmacol*, 2000, **57**, 976–983.
21 M. Isemura, T. Mita, K. Satoh, K. Narumi and M. Motomiya, *Cell BiologyInternational Reports*, 1991, **15**, 965–972.
22 M. Kovacs, J. Toth, C. Hetenyi, A. Malnasi-Csizmadia and J. R. Sellers, *J. Biol. Chem.*, 2004, **279**, 35557–35563.
23 B. Li, F. Li, H.-X. Li, X.-C. Xu, M. Szczodry, Z.-C. Yang, J.-S. Lin and J. H.-C. Wang, *Mol. Cell Biomech*, 2006, **3**, 225–227.
24 D. A. Lauffenburger and L. G. Griffith, *Proc. Natl. Acad. Sci. U. S. A.*, 2001, **98**, 4282–4284.
25 P. L. Ryan, R. A. Foty, J. Kohn and M. S. Steinberg, *Proc. Natl. Acad. Sci. U. S. A.*, 2001, **98**, 4323–4327.
26 A. K. Harris, *J. Theor. Biol.*, 1976, **61**, 267–285.
27 M. Krieg, Y. Arboleda-Estudillo, P. H. Puech, J. Kafer, F. Graner, D. J. Muller and C. P. Heisenberg, *Nat. Cell Biol.*, 2008, **10**, 429–436.
28 M. S. Steinberg, *Science*, 1963, **141**, 401–408.
29 G. W. Brodland and H. H. Chen, *J. Biomech.*, 2000, **33**, 845–851.
30 A. J. Engler, S. Sen, H. L. Sweeney and D. E. Discher, *Cell*, 2006, **126**, 677–689.
31 S. Huang and D. E. Ingber, *Exp. Cell Res.*, 2000, **261**, 91–103.
32 L. E. Dike, C. S. Chen, M. Mrksich, J. Tien, G. M. Whitesides and D. E. Ingber, *In Vitro Cell. Dev. Biol.: Anim.*, 1999, **35**, 441–448.
33 J. L. Charest, J. M. Jennings, W. P. King, A. P. Kowalczyk and A. J. Garcia, *J. Invest. Dermatol.*, 2009, **129**, 564–572.